

Analysis of Structural Units and Their Influence on Thermal Degradation of Alkali Lignins

Wen Hua, Chao Liu, Shu-bin Wu,* and Xiao-hong Li

The chemical structures of four alkali lignins isolated from poplar, fir, straw, and bagasse were investigated. To explore the relationship between the structural units and the thermal decomposition behavior, the system was tested by elemental analysis, Fourier transform infrared spectrometry, thermogravimetric analysis (TGA), and pyrolysis-gas chromatography/mass spectrometry (Py-GC/MS). The results indicated that the carbon content of poplar lignin (PL) was higher than that of others. Fir lignin (FL) exhibited the highest guaiacol units, while the other three lignins were abundant in syringol units. The thermal decomposition characteristics and pyrolysis products of the four lignins were influenced by the material structural and composition. The DTG curves showed that the initial temperatures and major degradation temperatures of woody lignins (FL and PL) with complex inherent structures were shifted to the high temperature zone compared with that of non-woody (BL and SL) lignins. Py-GC/MS analysis showed that guaiacol-type phenolic compounds were predominant pyrolysis products derived from the four lignins. The yield of guaiacol-type phenols could reach 82.87%. Moreover, the BL had selectively on phenol-type compounds with yield of 27.89%.

Keywords: Alkali lignin; Chemical structural unit; Thermal degradation analysis; Py-GC/MS

Contact information: State Key Laboratory of Pulp and Paper Engineering, South China University of Technology, Guangzhou, Guangdong 510640, PR China; *Corresponding author: shubinwu@scut.edu.cn

INTRODUCTION

With the increasing global energy crisis and environmental deterioration, speeding up the development of new green energy has become an urgent task and has attracted the whole world's attention (Hrayshat 2007; Ounas *et al.* 2011). Biomass, one form of renewable and clean energy, has advantages such as low pollution, wide distribution, and a large scale of reserves. Thus, biomass is considered a sustainable energy source that can be a substitution for fossil fuels. As existing infrastructures require hydrocarbons for manufacturing goods, such a substitution capability would allow the reuse of existing petrochemical industry infrastructures to produce petroleum-like products (Serrano-Ruiz and Dumesic 2011; Dickerson and Soria 2013). As one of the main components in lignocellulose biomass (accounting for 18 to 40 wt.%), lignin is one of the only non-petroleum resources that can provide renewable aryl compounds in nature. Compared to cellulose and hemicellulose, lignin is a random, amorphous polymer and has a complicated three-dimensional polymeric structure (Cateto *et al.* 2008; Kawamoto *et al.* 2008). Currently, industrial lignin primarily comes from the pulp and papermaking industry through soda pulping process, and the production could reach 50 million tons per year globally (Lora and Glasser 2002). However, the lignin dissolved in the black liquor has mostly been used directly for combustion as a fuel, which means that the high value-added

utilization of lignin has not been completely achieved yet (Ragauskas *et al.* 2014).

In past decades, many studies have reported biomass utilization, in which thermochemical conversion of biomass has become a hot-spot of research. Pyrolysis is touted to be one of the most promising thermochemical technologies, with the potential to transform biomass into fuels, synthetic gas, and some value-added chemicals (Jenkins *et al.* 1998). A series of reactions occur in a pyrolysis process, which is an extremely complex process, and the reactions could be influenced by many factors. Consequently, fundamental studies of biomass pyrolysis can lead to a better understanding of such processes (Yang *et al.* 2007; Dickerson and Soria 2013; Lv *et al.* 2013; Liang *et al.* 2015). The chemical structure of lignin can vary widely because of the diverse original materials and the isolation methods, which have a distinct influence on the thermal degradation behaviors and production distribution of the pyrolysis process (Li 2002; Jiang *et al.* 2010). Bagasse lignin has been studied, and it was found that bagasse enzymatic hydrolysis/mild acidolysis lignin (EMAL) is formed by the phenolic hydroxyl group of guaiacol and syringol units and the decomposition characteristics of EMAL were much different from that of bagasse under elevated temperatures (Wu *et al.* 2006). The chemical structure and the thermal degradation of Chinese fir kraft lignin and maple kraft lignin were compared using FTIR, TG-FTIR, and Py-GC/MS (Zhao *et al.* 2014). The results indicated that maple lignin contained more methoxyl groups and syringol-type units than Chinese fir lignin, and more phenol-type compounds were released from Chinese fir lignin pyrolysis than from maple lignin. Manchurian ash Bjorkman lignin and Mongolian Scots pine Bjorkman lignin were investigated using TG-FTIR (Wang *et al.* 2009). Manchurian ash lignin showed a higher thermal degradation rate and had higher residue yields than Mongolian Scots pine lignin. It should be clear that the composition of the pyrolysis oil, and the structure of the hardwood, softwood, and non-wood lignins, have not been systematically studied, resulting in limitations in understanding the transformation of aromatic compounds.

The present work systematically investigates the thermal decomposition behaviors of four alkali lignins (poplar, fir, straw, and bagasse) to explore the differences in the material properties, so that the pulping black liquor through pyrolysis can be efficiently utilized in the field of energy. The chemical structure characteristics of the four lignins were explored by elemental analysis and FTIR. Meanwhile, the thermal decomposition characteristics and pyrolysis products of the four lignins were examined by TGA and Py-GC/MS.

EXPERIMENTAL

Materials

The four alkali lignins isolated from the black liquors through the soda pulping in our laboratory (Li and Wu 2014) were poplar lignin (PL), fir lignin (FL), straw lignin (SL), and bagasse lignin (BL). The extraction process of lignins included mild acidolysis which put dilute acid solution into black liquor in order to adjust the pH to 2.0. Then the precipitated lignin was centrifuged, subjected to dioxane extraction, and partially dried in a rotary evaporator to a syrup-like solution.

The thickened solution was dropped into acidified deionized water, centrifuged to precipitate the lignin, and the obtained lignin was washed with HPLC grade hexane and

dried in a vacuum oven at room temperature (Liu *et al.* 2014). After the above process, the lignin materials had become very pure with no ash and no water.

Methods

Elemental analysis

The C, H, N, and S contents in lignin samples were obtained using a Vario-EL CUBE elemental analyzer (ELEMENTAR, Germany). The oxygen content was obtained by the difference method. The molecular formula was determined from the atomic ratio of C, H, O, and N.

FTIR

The chemical information regarding the distribution of monomeric units and typical functional groups of lignin samples were measured by a FTIR (Nexus Thermo Nicolet, USA) device in the range of 4000 to 400 cm^{-1} with a resolution of 4 cm^{-1} using a KBr disc containing 1% of finely ground samples.

TG/DTG

Thermal performances of the four lignins were produced by a STA449 F3 Jupiter thermogravimetric analyzer (Netzsch, Germany). High-purity nitrogen (99.99%) was the carrier gas, with a flow rate of 40 mL/min. In each experiment, approximately 10 mg of lignin sample was placed in the ceramic crucible and heated from room temperature to 800 °C at a heating rate of 20 °C/min. The system could automatically collect the weight loss data.

Pyrolysis methods

Flash pyrolysis experiments of lignin samples were carried out with Py-GC/MS. A flash pyrolyzer (CDS 5250, CDS Analytical, USA) was connected to a gas chromatograph (7890A, Agilent Technologies, USA) and coupled with a mass spectrometer (5975C, Agilent Technologies, USA). Approximately 0.2 mg of lignin sample was pyrolyzed at 600 °C for 15 s with a heating rate of 10 °C/ms. High-purity He was used as the carrier gas, with a flow rate of 1.00 mL/min, and the split ratio was 50:1. The evolved volatiles were identified by GC/MS with the following conditions: the injector temperature was kept at 300 °C; the GC oven was programmed from 50 to 250 °C at a rate of 8 °C/min and held for 5 min.

The chromatographic separation was performed with a HP-5MS (30 m, 0.25-mm inner diameter, 0.25- μm film thickness) capillary column; and the mass spectra were operated in electron ionization (EI) mode at 70 eV. The mass spectra were obtained from m/z 45 to 500.

The yield of the compounds can be determined by the characterized GC/MS spectrums, according to the Perkin Elmer (USA) NIST Spectral Version 5 software and other previous reports (del Río *et al.* 2011; Jiang *et al.* 2010). Lignin-derived monomeric products were identified based upon retention time and use of mass spectral libraries. Quantitative determination was carried out in relative terms using integration of the gasization peak area (Maldhure and Ekhe 2013).

RESULTS AND DISCUSSION

Chemical Structure of Alkali Lignins

The elemental content, the higher heating value (HHV), the atomic ratio of O/C and H/C, and the empirical formulas of the four lignins are summarized in Table 1. Regarding the H/C ratio among the four alkali lignins, the value of BL was the highest, which suggests that the BL was more beneficial to obtain high-quality bio-oil. Sulfur content was observed in BL and SL, but had no noticeable negative effects on the pyrolysis products according to the Py-GC/MS experiment (Table 3). The HHVs of FL, PL, and BL were 25.14, 25.06, and 26.78 MJ/kg, respectively, noticeably higher than that of SL. This suggests that the bio-oil derived from FL, PL, and BL may be beneficial for the formation of high-quality bio-oil and energy-oriented utilization.

Table 1. Elemental Analysis of the Four Alkali Lignins

Substrates	Elements (wt.%).					O/C ^b	H/C ^b	HHV ^c (MJ/Kg)	Empirical formula
	C	H	O ^a	N	S				
FL	65.03	5.85	29.03	0.09	-	0.33	1.08	25.14	C ₁₀ H _{10.79} O _{3.35} N _{0.01}
PL	64.05	6.11	29.73	0.11	-	0.35	1.14	25.06	C ₁₀ H _{11.44} O _{3.48} N _{0.015}
BL	64.30	6.87	27.34	0.32	1.17	0.32	1.28	26.78	C ₁₀ H _{12.82} O _{3.19} N _{0.04}
SL	62.13	5.94	29.37	0.84	1.72	0.35	1.15	24.39	C ₁₀ H _{11.47} O _{3.55} N _{0.12}

^a Calculated by difference

^b As atomic ratio

^c Calculated according to the Dulong formula (Yuan *et al.* 2009)

The FTIR spectra of the four alkali lignins are shown in Fig. 1, and the notable peak assignments can be referenced from previous studies (Tahmli *et al.* 1999; Sun *et al.* 2005; Ounas *et al.* 2011; Lv *et al.* 2013; Prinsen *et al.* 2013). The absorbance of peak 1 located at (3420 cm⁻¹) was due to the O-H stretching vibration, in which the absorption area of the four lignins was relatively large, showing that the four lignins were all abundant in the O-H group. Peak 2 (2936 cm⁻¹) indicated the notable C-H stretching vibration in methyl, methylene, and methyne groups; and C-H bending vibration in methyl groups can be assigned to peak 7 (1460 cm⁻¹). The absorbance in the range of 1725 to 1705 cm⁻¹ (peak 4) represents the C=O in unconjugated carbonyls stretching. At this peak, the absorption intensity of wood lignin was relatively higher than that of non-wood lignin, meaning that the wood alkali lignin contained more carboxyl groups than non-wood alkali lignin after cooking. The appearance of carbonyl groups at peak 5 (1604 cm⁻¹) showed that the C=O bond was in conjugation with the aromatic ring. The stretching signal at 1513 cm⁻¹ (peak 6) corresponds to the existence of skeleton stretching vibration of the benzene ring, which is the characteristic absorption peak of lignin. The four alkali lignins had strong absorption, but the peaks of FL and PL were even stronger than those of BL and SL, which indicated that the benzene skeleton structure had not been destroyed and further suggested that the structure of wood lignin was more stable than that of non-wood lignin in the cooking process. The signal at 1329 cm⁻¹ (peak 8) showed that three of the four lignins (except FL) included a certain content of syringol and guaiacol rings on five condensation units. The absorbance of peak 10 (1115 cm⁻¹) can be ascribed to the C-H stretching vibration in a syringol-type ring. Stronger absorption signals appeared in PL, SL, and BL, while no

visible absorbance can be found in FL, which is consistent with previous studies and confirms the rich content of syringol-type units in PL, SL, and BL (Ibarra *et al.* 2005; Zhao *et al.* 2014). This is also in accordance with the Py-GC/MS results that follow. Peaks at 1270 cm^{-1} , assigned to C-O, and at 1150 cm^{-1} , ascribed to C-H stretching vibration in guaiacol rings, appear in PL and FL, while no obvious absorption can be found in BL and SL.

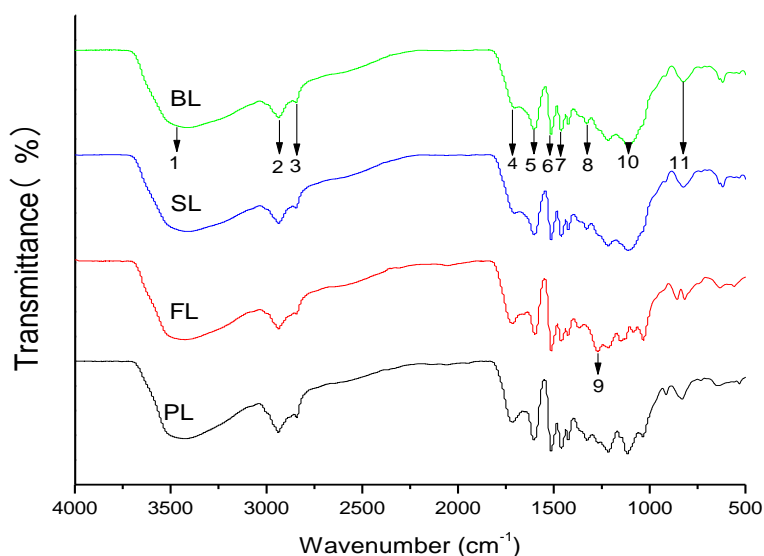


Fig. 1. FTIR spectra of the four alkali lignins

Thermogravimetric Properties of Alkali Lignins

The TG and DTG curves of the four alkali lignins are plotted in Fig. 2. The results indicate that the major weight loss stage of the four lignins was distinct and the decomposition of lignin could be divided into three stages. The first stage occurred before $120\text{ }^{\circ}\text{C}$ and involved primarily physical changes, including the dehydration and small impurity molecule volatilization process (Xiao *et al.* 2001). The second stage took place from 120 to $280\text{ }^{\circ}\text{C}$. In this process, the alkali lignin began to degrade, mostly because of the depolymerization or "glass transition" of alkali lignin was a slow process. The third stage (280 to $550\text{ }^{\circ}\text{C}$) was the active stage of the lignin polymer pyrolysis. It was attributed to the intensive evolution of volatiles. The thermogravimetric experiment suggested that the decomposition took place in a wide temperature range (approximately 120 to $550\text{ }^{\circ}\text{C}$). This may occur because lignin contains many aromatic rings with various branches; the activity of the chemical bonds and functional groups of lignin possess an extremely wide rupture range (Gu *et al.* 2013), which may also influence the results.

The initial thermal degradation temperature, maximum devolatilization rate temperature, and the yield of charred residues are summarized in Table 2. The initial degradation temperatures of PL and FL were higher than those of SL and BL. This is probably due to the higher degree of polymerization and molecular weight of wood alkali lignin (Parthasarathy *et al.* 2013; Li and Wu 2014). The maximum devolatilization rate temperatures of the four alkali lignins were $403\text{ }^{\circ}\text{C}$ for PL, $411\text{ }^{\circ}\text{C}$ for FL, $336\text{ }^{\circ}\text{C}$ for SL, and $383\text{ }^{\circ}\text{C}$ for BL. These results suggested that the four alkali lignins had differences in

their inherent structures and chemical natures (this can be seen from the FTIR data, in which PL and FL had higher contents of guaiacol groups and FL has no syringol group), which may influence the degradation characteristics of lignin to a large extent. Previous studies have demonstrated that the connection between lignin macromolecules mostly involves ether bonds, and the ether bonds between guaiacol units are more stable than those between syringol units, which may explain why FL has the highest maximum devolatilization rate temperature (Jakab *et al.* 1997). A large amount of lignin remained after 800 °C because of its condensation or relocation. There were about 35% charcoal residues in PL, FL, and BL. However, the value of charcoal residue in SL reached 47.79%. This was because the straw structure contained more inorganic matter and ashes, which is the main reason for the high residual content. Excluding ash, the charcoal residue may be attributed to the presence of inorganic mineral contents (Wang *et al.* 2009). Thus, these results may suggest that PL, FL, and BL are more suitable than SL for bio-oil production by pyrolysis.

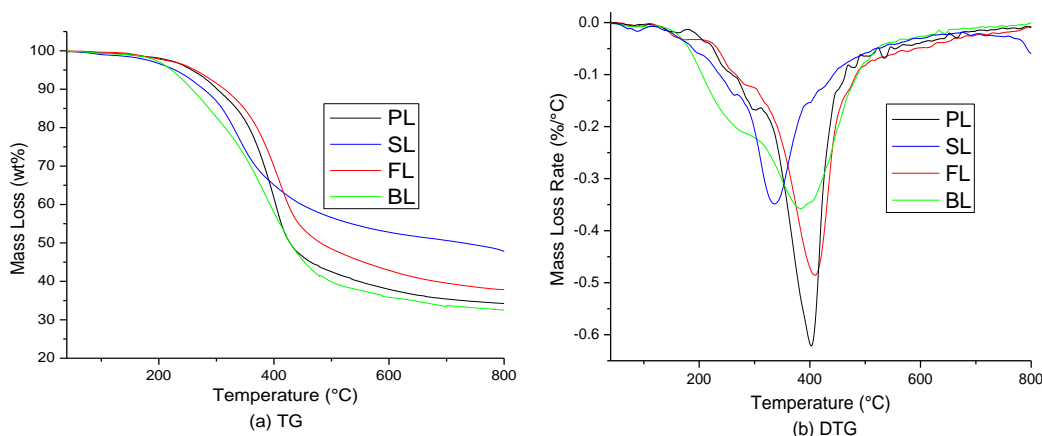


Fig. 2. TG and DTG curves of the four alkali lignins

Table 2. Thermogravimetric Analysis of the Four Alkali Lignins

Component	Initial temperature ^a (°C)	Major degradation temperatures (°C)	Degradation at 200-550 °C (%)	Char residue (%)
PL	218	403	58.17	34.24
FL	212	411	52.80	37.84
SL	182	336	42.26	47.79
BL	194	383	59.41	30.64

^a The initial temperature assumed to correspond to the dry sample mass fraction equal to 0.975.

Pyrolysis Bio-Oil from Alkali Lignins

Previous studies have confirmed that alkali lignin pyrolysis at 600 °C could obtain the maximum yields of phenolic compounds, while the yields of heterocyclic compounds, esters, and acid compounds are at a minimum. The phenolic compounds are important organic synthetic materials and chemical raw materials that can be used to produce

phenolics, synthetic fibers, fuels, dyes, and pesticides. Therefore, we adopt a pyrolysis temperature of 600 °C.

Figure 3 shows the distribution of typical aromatic compounds (guaiacol-type, syringol-type, phenol-type, catechol-type, and other aromatic compounds) from fast pyrolysis of the four alkali lignins at 600 °C. Based on the total ion flow chart, the relative content of each peak was calculated using an area normalization method, and qualitative analysis was carried out for the products as well. The different contents of guaiacol-type, syringol-type, and phenol-type compounds in the pyrolysis products roughly reflect the fact that the PL, FL, BL, and SL had different chemical structure and pyrolysis properties. Figure 3 shows that guaiacol-type compounds were the dominant products of the four alkali lignins, among which they accounted for 50.26% (PL), 82.87% (FL), 38.94% (BL), and 35.26% (SL), respectively. This can be attributed to their basic structure, which is primarily composed of guaiacol propane. Furthermore, the main types of inter-unit linkages in alkali lignin are β -O-4, α -O-4, and 4-O-5 bonds, which could easily produce guaiacol in the lignin degradation process. The production of syringol-type compounds obtained from SL pyrolysis was 31.44%, which was significantly higher than that of the other three alkali lignins. This result indicates that the SL had a more syringol-type structure compared with the others, in line with the fact that the SL contained more syringol units in the above FTIR analysis. More phenol-type compounds were released from BL, PL, and SL than from FL. This was mostly due to the presence of phenol-type structural units of bagasse, polar, and straw alkali lignin. Moreover, previous studies have shown that phenol-type compounds can be produced not only from cracking phenol units, but also from the cleavage of the ArO-CH₃ of guaiacol units at 600 °C (Zhao *et al.* 2014). The cresol-type products were primarily produced in ArO-CH₃ bond fracture. In the pyrolysis products of fir alkali lignin, the yield of phenol-type compounds less than that of catechol-type compounds probably occurred because the Ar-OCH₃ bond breaking energy (416.7 kJ/mol) was greater than that of ArO-CH₃ (273.0 kJ/mol).

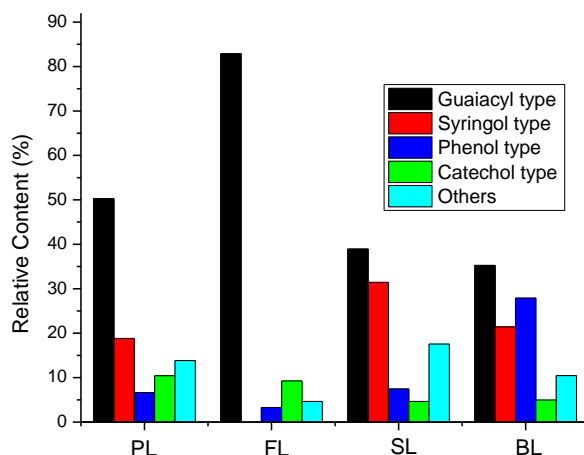


Fig. 3. Distribution of the typical fast pyrolysis products of four alkali lignins

The identification and relative molar abundance of the released compounds from the four alkali lignin pyrolysis are shown in Table 3. 4-Hydroxy-3-methoxybenzoic acid (G10, 11.61%) was the predominant guaiacol-type product for PL; 2-methoxy-4-methylphenol (G2, 15.98%) was the most common guaiacol-type outcome for FL; 2-

methoxyphenol (G1, 10.80%) and 4-ethyl-2-methoxyphenol (G4, 10.59%) dominated the guaiacol-type products for SL and BL, respectively. It can be found that apart from FL, the yield of syringol (2,6-dimethoxyphenol) was the highest of the syringol-type compounds for the other three alkali lignins, in which the productivity of syringol accounted for 17.07% for BL. This is much higher than the other alkali lignins, implying that BL had a higher selectivity of syringol formation at 600 °C because of its rich syringol-type C9 units. 4-Ethenylphenol (H5 in Table 4) was found only in non-wood lignins, mostly from the demethoxylation of 2-methoxy-4-vinylphenol. It may be deduced that compared with wood lignin, non-wood lignin is more likely to exhibit a demethoxylation reaction. 3-Methoxy-1,2-benzenediol was the most prominent product among the catechol-type compounds in PL, BL, and SL, probably because of the demethoxylation of 2,6-dimethoxyphenol or demethylation of guaiacol.

Table 3. Pyrolysis Products from the Four Alkali Lignins at 600 °C

No. ^a	Compounds	Formula	PL	FL	SL	BL
G1	Phenol, 2-methoxy-	C ₇ H ₈ O ₂	3.20	13.07	10.80	4.72
G2	Phenol, 2-methoxy-4-methyl-	C ₈ H ₁₀ O ₂	10.06	15.98	2.32	2.63
G3	2-Methoxy-6-methylphenol	C ₈ H ₁₀ O ₂	3.78	8.07	2.12	1.87
G4	Phenol, 4-ethyl-2-methoxy-	C ₉ H ₁₂ O ₂	4.70	11.22	9.83	10.59
G5	2-Methoxy-4-vinylphenol	C ₉ H ₁₀ O ₂	0.75	1.58	0.43	0.91
G6	eugenol	C ₁₀ H ₁₂ O ₂	3.51	1.97	-	0.46
G7	Phenol, 2-methoxy-4-propyl-	C ₁₀ H ₁₄ O ₂	0.80	1.58	0.72	-
G8	Vanillin	C ₈ H ₈ O ₃	1.66	10.54	1.56	1.47
G9	Phenol, 2-methoxy-4-(1-propenyl)-, (Z)-	C ₁₀ H ₁₂ O ₂	0.73	1.52	0.53	0.71
G10	Benzoic acid, 4-hydroxy-3-methoxy-	C ₈ H ₈ O ₄	11.61	-	3.07	3.44
G11	Phenol, 2-methoxy-4-(1-propenyl)-, (E)-	C ₁₀ H ₁₂ O ₂	3.95	4.40	2.41	3.59
G12	Ethanone, 1-(4-hydroxy-3-methoxyphenyl)-	C ₉ H ₁₀ O ₃	3.02	5.44	2.41	2.26
G13	2-Propanone, 1-(4-hydroxy-3-methoxyphenyl)-	C ₁₀ H ₁₂ O ₃	1.28	0.83	1.37	0.77
G14	4-hydroxy-3-methoxycinnamic acid	C ₁₀ H ₁₀ O ₄	1.04	-	0.44	0.69
G15	Benzeneacetic acid,4-hydroxy-3-methoxy,methyl ester	C ₁₀ H ₁₂ O ₄	0.19	0.59	-	-
G16	4-((1E)-3-Hydroxy-1-propenyl)-2-methoxyphenol	C ₁₀ H ₁₂ O ₃	-	-	0.94	0.62
G17	Homovanillyl alcohol	C ₉ H ₁₂ O ₃	-	6.07	-	0.53
	Total		50.26	82.87	38.94	35.26
S1	Phenol, 2,6-dimethoxy-	C ₈ H ₁₀ O ₃	7.74	-	17.07	7.40
S2	Phenol, 2,6-dimethoxy-4-(2-propenyl)-	C ₁₁ H ₁₄ O ₃	4.97	-	3.00	5.82
S3	Benzaldehyde, 4-hydroxy-3,5-dimethoxy-	C ₉ H ₁₀ O ₄	3.18	-	2.21	2.41
S4	Ethanone, 1-(4-hydroxy-3,5-dimethoxyphenyl)-	C ₁₀ H ₁₂ O ₄	2.22	-	7.17	3.60
S5	Benzoic acid, 4-hydroxy-3,5-dimethoxy-	C ₉ H ₁₀ O ₅	0.45	-	1.98	1.46
S6	3,5-Dimethoxy-4-hydroxycinnamaldehyde	C ₁₁ H ₁₂ O ₄	0.26	-	-	0.75
	Total		18.82	0.00	31.44	21.43
H1	Phenol	C ₆ H ₆ O	-	0.05	3.13	1.46
H2	Phenol, 4-methyl-	C ₇ H ₈ O	0.23	0.52	0.60	1.13
H3	Phenol, 2-methyl-	C ₇ H ₈ O	0.34	0.92	0.58	0.37
H4	Phenol, 4-ethyl-	C ₈ H ₁₀ O	-	-	0.78	1.65
H5	Phenol, 4-ethenyl	C ₈ H ₈ O	-	-	1.88	20.18
H6	Phenol, 2,4-dimethyl-	C ₈ H ₁₀ O	0.43	1.76	-	-
H7	3-Methoxy-5-methylphenol	C ₈ H ₁₀ O ₂	0.92	-	-	0.49

H8	Phenol, 3,4-dimethoxy-	C ₈ H ₁₀ O ₃	4.72	-	0.46	1.44
H9	<i>p</i> -Isopropenylphenol	C ₉ H ₁₀ O	-	-	-	0.48
H10	Phenol, 4-(2-propenyl)-	C ₉ H ₁₀ O	-	-	-	0.46
H11	2-Allylphenol	C ₉ H ₁₀ O	-	-	-	0.24
	Total		6.64	3.25	7.44	27.89
CA1	1,2-Benzenediol	C ₆ H ₆ O ₂	1.24	4.60	0.80	0.62
CA2	1,2-Benzenediol, 3-methoxy-	C ₇ H ₈ O ₃	7.35	-	3.84	3.71
CA3	1,2-Benzenediol, 4-methyl-	C ₇ H ₈ O ₂	1.83	4.65	-	0.62
	Total		10.42	9.25	4.63	4.96
OT1	3,4-Dimethoxytoluene	C ₉ H ₁₂ O ₂	0.27	2.27	0.34	-
OT2	Propanal, 2-methyl-3-phenyl-	C ₁₀ H ₁₂ O	1.31	-	-	-
OT3	4-Ethoxy-3-anisaldehyde	C ₁₀ H ₁₂ O ₃	1.50	2.11	0.27	-
OT4	4-Propyl-1,1'-diphenyl	C ₁₅ H ₁₆	2.74	-	0.24	0.38
OT5	Benzene, 1,2,3-trimethoxy-5-methyl-	C ₁₀ H ₁₄ O ₃	4.17	-	1.88	1.30
OT6	1-Butanone, 1-(2,4,6-trihydroxy-3-methylphenyl)-	C ₁₁ H ₁₄ O ₄	1.74	-	7.22	3.60
OT7	4'-Phenylpropiophenone	C ₁₅ H ₁₄ O	1.23	-	0.54	-
OT8	Benzenepropanoic acid,4'-phenyl-	C ₁₅ H ₁₄ O ₂	0.89	-	-	-
OT9	4-Methyl-2,5-dimethoxybenzaldehyde	C ₁₀ H ₁₂ O ₃	-	-	6.65	4.82
OT11	Ethanone, 1-(3,4,5-trimethoxyphenyl)-	C ₁₁ H ₁₄ O ₄	-	-	0.40	-
OT12	Benzene, 1,1'-propylidenebis-	C ₁₅ H ₁₆	-	-	-	0.35
OT13	Benzene, 4-ethyl-1,2-dimethoxy-	C ₁₀ H ₁₄ O ₂	-	0.26	-	-
	Total		13.85	4.64	17.55	10.45

^a G: guaiacol-type compounds (G1-G17); S: syringol-type compounds (S1-S6); H: phenol-type compounds (H1-H11); Ca: catechol-type compounds (Ca1-Ca3); OT: other compounds (OT1-OT13)

CONCLUSIONS

1. Elemental analysis indicated that BL had the highest H/C ratio and FL had the highest HHV, which suggested that it could enhance the bio-oil quality. FTIR analysis showed that FL contained more guaiacol units, while other three alkali lignins were abundant in syringol units.
2. Thermogravimetric characteristics of the four lignins were influenced by their chemical structural significantly. The thermal decomposition of the four lignins could be divided into three stages (dehydrate, volatile releasing, and decomposition of lignin) basically ranging from 120 to 550 °C. Compared with SL, the residue yields of PL, FL, and BL were lower, suggesting that they were more suitable for bio-oil production through flash pyrolysis.
3. Py-GC/MS analysis showed that the selectivity of pyrolysis products could be improved by the different structural units of four lignins. Total guaiacol-type compounds derived from FL pyrolysis were highest, which they could reach 82.87%. BL pyrolysis obtained the highest yield of phenol-type compounds (27.89%).
4. 4-Hydroxy-3-methoxybenzoic acid (11.61%) was the dominant pyrolysis product of PL. The yields of syringol and 4-ethenylphenol derived from BL pyrolysis reached

17.07% and 20.18%, respectively, which is conducive to preparation of primary intermediates in the fine chemicals industry.

ACKNOWLEDGEMENTS

The authors greatly acknowledge the support of the National Basic Research Program of China (973 program, No. 2013CB228101), the Natural Sciences Foundation of China (No. 31270635 and No. 21176095), and the Fundamental Research Funds for the Central Universities (No. 2014ZP14).

REFERENCES CITED

- Cateto, C. A., Barreiro, M. F., Rodrigues, A. E., Brochier-Salon, M. C., Thielemans, W., and Belgacem, M. N. (2008). "Lignins as macromonomers for polyurethane synthesis: A comparative study on hydroxyl group determination," *Journal of Applied Polymer Science* 109(5), 3008-3017. DOI: 10.1002/app.28393.
- del Río, J. C., Rencoret, J., Gutiérrez, A., Nieto, L., Jiménez-Barbero, J., and Martínez, Á. T. (2011). "Structural characterization of guaiacyl-rich lignins in flax (*Linum usitatissimum*) fibers and shives," *Journal of agricultural and food chemistry* 59(20), 11088-11099. DOI: 10.1021/jf201222r
- Dickerson, T., and Soria, J. (2013). "Catalytic fast pyrolysis: a review," *Energies* 6(1), 514-538. DOI: 10.3390/en6010514.
- Gu, X. L., Ma, X., Li, L. X., Liu, C., Cheng, K. H., and Li, Z. Z. (2013). "Pyrolysis of poplar wood sawdust by TG-FTIR and Py-GC/MS," *Journal of Analytical and Applied Pyrolysis* 102, 16-23. DOI: 10.1016/j.jaap.2013.04.009.
- Hrayshat, E. S. (2007). "Analysis of renewable energy situation in Jordan," *Energy Sources, Part B: Economics, Planning, and Policy* 3(1), 89-102. DOI: 10.1016/S0146-6380(99)00120-5.
- Ibarra, D., del Río, J. C., Gutiérrez, A., Rodríguez, I. M., Romero, J., Martínez, M. J., and Martínez, Á. T. (2005). "Chemical characterization of residual lignins from eucalypt paper pulps," *Journal of Analytical and Applied Pyrolysis* 74(1-2), 116-122. DOI: 10.1016/j.jaap.2004.12.009.
- Jakab, E., Faix, O., and Till, F. (1997). "Thermal decomposition of milled wood lignins studied by thermogravimetry/mass spectrometry," *Journal of Analytical and Applied Pyrolysis* 40, 171-186. DOI: 10.1016/S0165-2370(97)00046-6.
- Jenkins, B. M., Baxter, L. L., Miles Jr., T. R., and Miles, T. R. (1998). "Combustion properties of biomass," *Fuel Processing Technology* 54(1-3), 17-46. DOI: 10.1016/S0378-3820(97)00059-3.
- Jiang, G. Z., Nowakowski, D. J., and Bridgwater, A. V. (2010). "A systematic study of the kinetics of lignin pyrolysis," *Thermochimica Acta* 498(1-2), 61-66. DOI: 10.1016/j.tca.2009.10.003.
- Kawamoto, H., Ryoritani, M., and Saka, S. (2008). "Different pyrolytic cleavage mechanisms of β -ether bond depending on the side-chain structure of lignin dimers,"

- Journal of Analytical and Applied Pyrolysis* 81(1), 88-94. DOI: 10.1016/j.jaap.2007.09.006.
- Li, J., L. B., Zhang, X. C. (2002). "Comparative studies of thermal degradation between larch lignin and manchurian ash lignin," *Polymer Degradation and Stability* 78(2), 279-285. DOI: 10.1016/S0141-3910(02)00172-6.
- Li, X. H., and Wu, S. B. (2014). "Chemical structure and pyrolysis characteristics of the soda-alkali lignin fractions," *BioResources* 9(4) 6277-6289. DOI: 10.15376/biores.9.4.6277-6289
- Liang, J. J., Lin, Y. Q., Wu, S. B., Liu, C., Lei, M., Zeng, C. (2015). "Enhancing the quality of bio-oil and selectivity of phenols compounds from pyrolysis of anaerobic digested rice straw," *Bioresource Technology* 181, 220-3. DOI: 10.1016/j.biortech.2015.01.056.
- Liu, C., Liang, J. J., Wu, S. B., and Deng, Y. B. (2014). "Effect of chemical structure on pyrolysis behavior of alcell mild acidolysis lignin," *BioResources* 10(1), 1073-1084. DOI: 10.15376/biores.10.1.1073-1084
- Lora, J. H., and Glasser, W. G. (2002). "Recent industrial applications of lignin: a sustainable alternative to nonrenewable materials," *Journal of Polymers and the Environment* 10(1-2), 39-48. DOI: 10.1023/A: 1021070006895.
- Lv, G. J., Wu, S. B., Yang, G. H., Chen, J. C., Liu, Y., and Kong, F. G. (2013). "Comparative study of pyrolysis behaviors of corn stalk and its three components," *Journal of Analytical and Applied Pyrolysis* 104, 185-193. DOI: 10.1016/j.jaap.2013.08.005.
- Maldhure, A. V., and Ekhe, J. (2013). "Pyrolysis of purified kraft lignin in the presence of AlCl₃ and ZnCl₂," *Journal of Environmental Chemical Engineering* 1(4), 844-849. DOI : 10.1016/j.jece.2013.07.026.
- Ounas, A., Aboukhas, A., El Harfi, K., Bacaoui, A., and Yaacoubi, A. (2011). "Pyrolysis of olive residue and sugar cane bagasse: Non-isothermal thermogravimetric kinetic analysis," *Bioresource Technology* 102(24), 11234-11238. DOI: 10.1016/j.biortech.2011.09.010.
- Parthasarathy, P., Narayanan, K. S., and Arockiam, L. (2013). "Study on kinetic parameters of different biomass samples using thermo-gravimetric analysis," *Biomass and Bioenergy* 58, 58-66. DOI: 10.1016/j.biombioe.2013.08.004.
- Prinsen, P., Rencoret, J., Gutiérrez, A., Liitiä, T., Tamminen, T., Colodette, J. L., Berbis, M.A., Jiménez-Barbero, J., Martínez, A. T., and del Río, J. C. (2013). "Modification of the lignin structure during alkaline delignification of eucalyptus wood by kraft, soda-AQ, and soda-O2 cooking," *Industrial & Engineering Chemistry Research* 52(45), 15702-15712. DOI: 10.1021/ie401364d.
- Ragauskas, A. J., Beckham, G. T., Biddy, M. J., Chandra, R., Chen, F., Davis, M. F., Davison, B. H., Dixon, R. A., Gilna, P., and Keller, M. (2014). "Lignin valorization: improving lignin processing in the biorefinery," *Science* 344(6185), 1246843. DOI: 10.1126/science.1246843
- Serrano-Ruiz, J. C., and Dumesic, J. A. (2011). "Catalytic routes for the conversion of biomass into liquid hydrocarbon transportation fuels," *Energy & Environmental Science* 4(1), 83-99. DOI: 10.1039/c0ee00436g.

- Sun, X. F., Sun, R. C., Fowler, P., and Baird, M. S. (2005). "Extraction and characterization of original lignin and hemicelluloses from wheat straw," *Journal of Agricultural and Food Chemistry* 53(4), 860-870. DOI: 10.1021/jf040456q.
- Tahmli, N., Mirzalar, F., Sirkecioglu, O., and Odabas, S. (1999). "Synthesis of new functional dioxepin polymers," *Reactive & Functional Polymers* 40(3), 289-293. DOI:10.1016/S1381-5148(98)00032-7.
- Wu, S. B., Guo, Y. L., Wang, S. G., Li, M. S. (2006). "Chemical structures and thermochemical properties of bagasse lignin," *Forestry Studies in China* 8(3), 34-37.
- Wang, S. R., Wang, K. G., Liu, Q., Gu, Y. L., Luo, Z. Y., Cen, K. F., and Fransson, T. (2009). "Comparison of the pyrolysis behavior of lignins from different tree species," *Biotechnology Advances* 27(5), 562-567. DOI:10.1016/j.biotechadv.2009.04.010.
- Xiao, B., Sun, X. F., and Sun, R. C. (2001). "Chemical, structural, and thermal characterizations of alkali-soluble lignins and hemicelluloses, and cellulose from maize stems, rye straw, and rice straw," *Polymer Degradation and Stability* 74(2), 307-319. DOI:10.1016/s0141-3910(01)00163-x.
- Yang, H. P., Yan, R., Chen, H. P., Lee, D. H., and Zheng, C. G. (2007). "Characteristics of hemicellulose, cellulose and lignin pyrolysis," *Fuel* 86(12-13), 1781-1788. DOI: 10.1016/j.fuel.2006.12.013.
- Yuan, X. Z., Tong, J. Y., Zeng, G. M., Li, H., and Xie, W. (2009). "Comparative studies of products obtained at different temperatures during straw liquefaction by hot compressed water," *Energy & Fuels* 23(6), 3262-3267. DOI: 10.1021/ef900027d
- Zhao, J., Wang, X. W., Hu, J., Liu, Q., Shen, D. K., and Xiao, R. (2014). "Thermal degradation of softwood lignin and hardwood lignin by TG-FTIR and Py-GC/MS," *Polymer Degradation and Stability* 108, 133-138. DOI: 10.1016/j.polymdegradstab.2014.06.006.

Article submitted: July 18, 2015; Peer review completed: September 6, 2015; Revised version received: October 1, 2015; Accepted: November 13, 2015; Published: January 12, 2016.

DOI: 10.15376/biores.11.1.1959-1970